ANALELE UNIVERSITĂŢII
“EFTIMIE MURGU” REŞIŢA
ANUL XXI, NR. 2, 2014, ISSN 1453 - 7397

Ion Voncilă, Răzvan Buhosu, Mădălin Costin

Topology Optimization of Switched Reluctance Motors to Increase Energy Efficiency

This paper proposes - and analyses in comparison – new topologies for switched reluctance motors (armature rotor thereof). The aim is to find a topology that minimizes losses and maximizes the torque developed by the SRM. For purposes of comparative analyse it is used PSIM software. Based on the results, conclusions are drawn regarding the design strategies of this type of electric machines in the near future.

Keywords: SRM, torque ripple, energy efficiency.

1. Introduction

Classic electric motors based on the electromagnetic induction principle are more and more difficult to use in the modern electric drives, which require shaft high sppeds, low time constants and high position control accuracies. Electromagnetic induction means to have to armatures equipped with ferromagnetic cores şi concentated and/or distributed windings. Volumetric extention of the ferromagnetic cores and of the the insulated windings towards these cores leads to large sizes of electric machines, high losses and, consequently, to short lifetimes. Shaft speed adjustment is difficult because the auxiliary systems are complex and is also expensive. That is why electric machines working on the principle of variable magnetic reluctance are used for applications of low and even medium power.

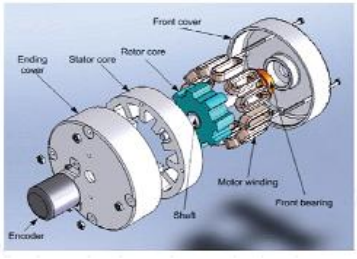

Figure 1. The construction of SRM

This type of electric machines has the advantage of a simple design (only one of the two armatures is equipped with winding, the stator), the speed can be adjusted on a large scale, and a high position control accuracy based on simple controls. Both simple design (usually the stator armature is equipped with salient poles and a concentrated winding supplied sequentially by a source of DC to the so called switched reluctance motor), the flexibility of rotor topology (design type gear), allow both low sizes and low losses within the structure (fig. 1) [1].

There are two ways of progress for these motors today: increase of the number of stator phases (Fig. 2) and use of new control strategies (supply of two phases simultaneously) [2], [3], respectively, change of rotor technology and, consequently, assume of new structural concepts (modular structures) [4], [5]. All these have an important purpose: increase of the electromagnetic torque (as medium value) and decrease of ripples of the electromagnetic torque curve.

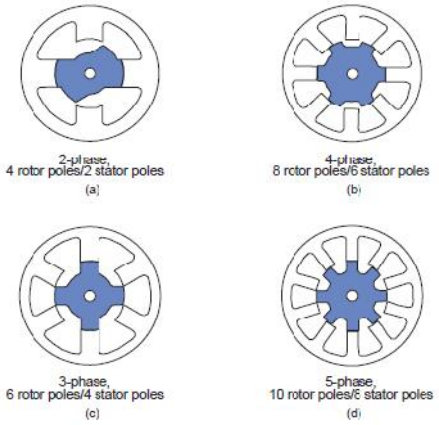

Figure 2. Various SRM geometries

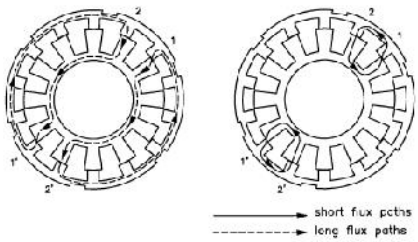

Figure 3. Excitation patterns in the 7—phase motor

It is obvious that the number of phases cannot be incresed very much, for purposes of size, but especially of simple design of control module. That is why notable performances for SRM can be obtained only by changing rotor geometry. Since the torque highly depends on the inductivities ratio of the positions aligned and non-aligned of the rotor teeth towards the stator poles it has to be found the specific topology so as to assure the best value of the torque related to a high value of motor energetic effiency through a convenient inductivities ratio. The paper deals with a comparative analysis between various topologies that assure a variation of inductivities ratio ($L_{\max} / L_{\min}$) on a large scale precisely to be able to see the influence of this ratio both on the medium value of electromagnetic torque, on torque ripples and shaft speed and on SRM energetic efficiency.

2. SRM Running and performance characteristics. Comparative analysis

PSIM software was used in order to perform the comparative analysis and to emphasize the influence of the phenomenon of shape anisotropy on the SRM running and performance characteristics.

The equation of phase voltages of the motor is:

$$u = Ri + \frac{d\Phi(\theta, i)}{dt} \tag{1}$$

where: R is the resitance of a stator phase, i is the current through the winding, Φ the total magnetic flux, u the supply voltage, and θ the position rotor angle.

The total magnetic flux is: $\Phi(\theta, i) = L(\theta, i) \cdot i$, where inductivity L depends on the rotor position and the value of phase current.

The instantaneous electromagnetic torque discharged by this motor is:

$$m = \frac{1}{2} \cdot \frac{\partial L}{\partial \theta} \cdot i^2 . \tag{2}$$

As a consequence of the above, it is clear that the torque does not depend on the current sense, it only depends on the inductivity variation with rotor position towards the stator, which depends on machine parameters, such as the number of stator and rotor poles and their topology.

The simplifying assumption accepted for modeling is that the inductivity variation towards rotor position is linear between the aligned, respectively non-aligned of rotor teeth towards the stator poles. It is also assumed that the inductivity value is not influenced by the value of stator winding current (as variation).

The schematic diagram used in PSIM is given in Fig. 4.

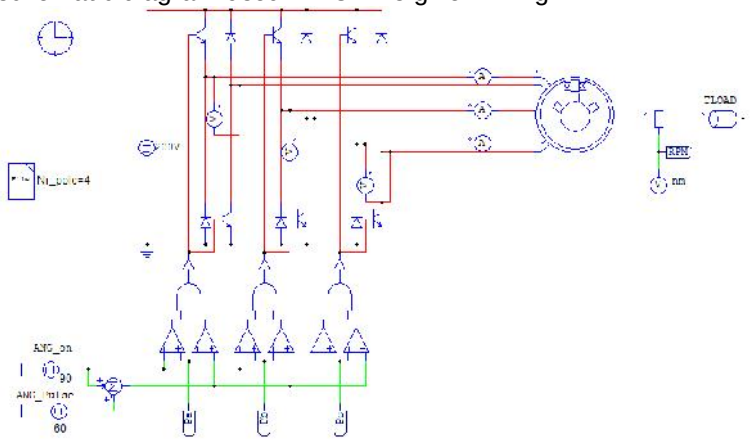

a)

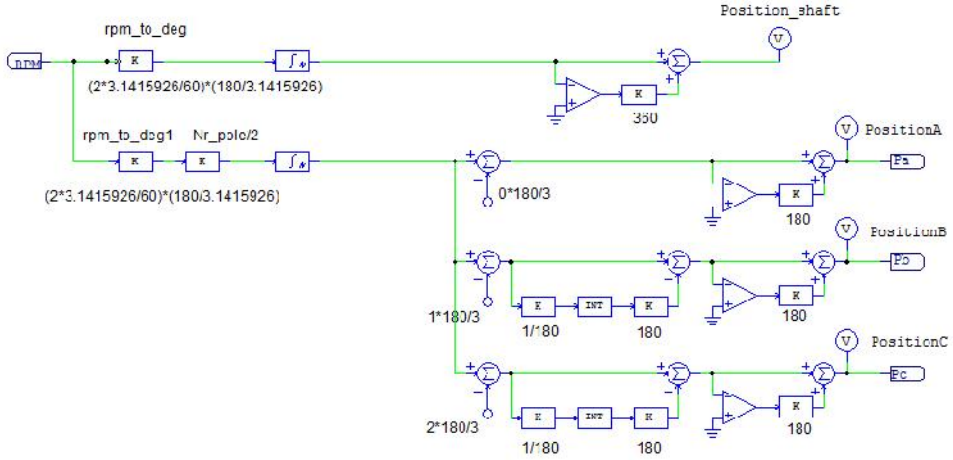

b)

Figure 4. Three Phase Switched Reluctance Motor Drive System [6]
a) force scheme; b) control scheme

The SRM behavior is analized in a range of variation of inductivities ratio (between 5 and 50) and to various shaft loads (for a variation of the resistant torque between 0,1 Nm and 3 Nm).

In the Fig. 5 are given the SRM parameters from PSIM library, which were the reference for the comparative analysis performed in this paper.

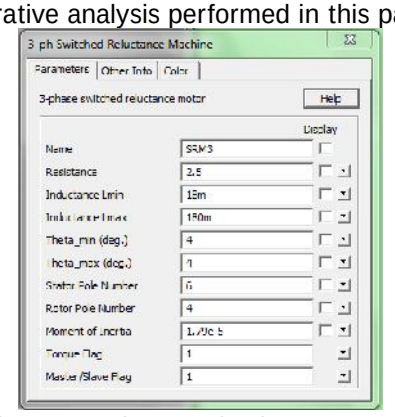

Figure 5. The SRM basic parameters

3. Resuts and discussions

The simulations aimed the following points: a) the value of the medium torque discharged for a certain inductivities ratio $L_{\max} / L_{\min}$ and implicitly, a certain SRM topology; b) the medium speed discharged at shaft, for a given ratio

L_{max} / L_{min} ; ripples value of the shaft speed curves and of electromagnetic torque discharged, for a given ratio L_{max} / L_{min} ; the values of electromechanic conversion efficiency, for a given ratio L_{max} / L_{min} .

The results obtained are shown below.

A. The case $\frac{L_{max}}{L_{min}} = 10$ - reference

Fig. 6 and 7 show current variations, respectively, voltage coresponding to a stator phase (the SRM analized has three pases), for a shaft load with a resistant torque of 1 Nm.

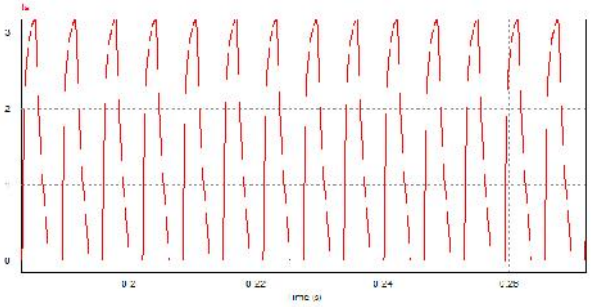

Figure 6. Current variation in the stator winding (zoom)

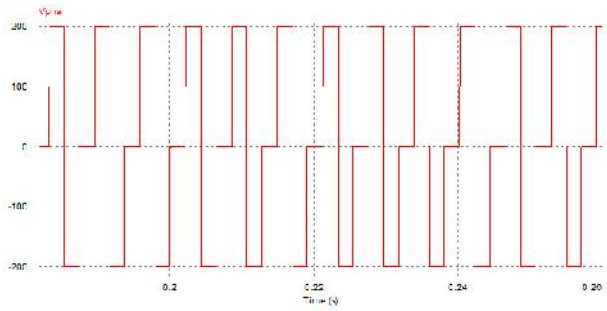

Figure 7. Voltage variation at the clamps of a stator phase (zoom)

Fig. 8 and 9 show both shaft speed variations, respectively electromagnetic torque variations for a resistant torque of 1 Nm and the ripples of the variation curves of these parameters.

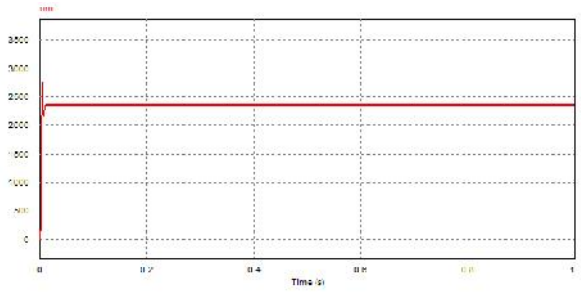

a)

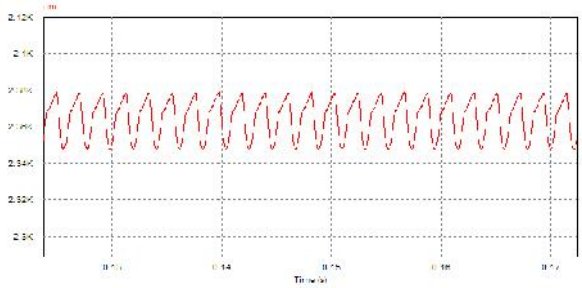

b)

Figure 8. Shaft speed variation, for the SRM analized, in the case of a resistant torque of 1 Nm (a) and the ripples of the shaft speed curve (b)

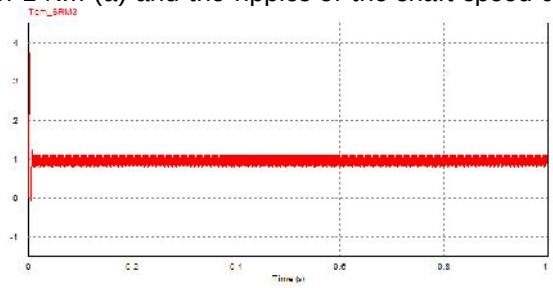

a)

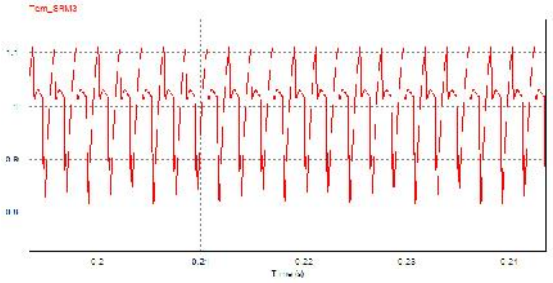

b)

Figure 9. Electromagnetic torque variation for the SRM analized, in the case of a resistant torque of 1 Nm (a) and the ripples of electromagnetic torque curve (b)

B. The case $\frac{L_{\max}}{L_{\min}} = 5$

Fig. 10 and 11 show both shaft speed variations, respectively, electromagnetic torque variations for a resistant torque of 1 Nm - and the ripples of the variation curves of these parameters, for the new topology, respectively, the new inductivities ratio.

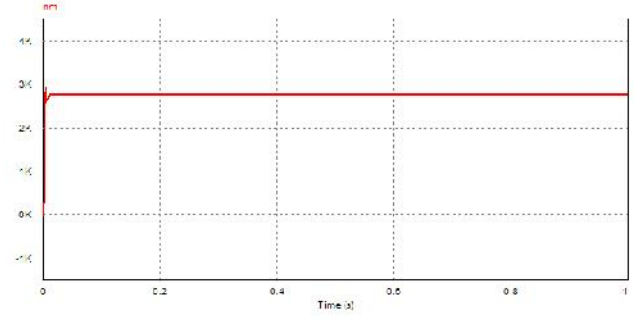

a)

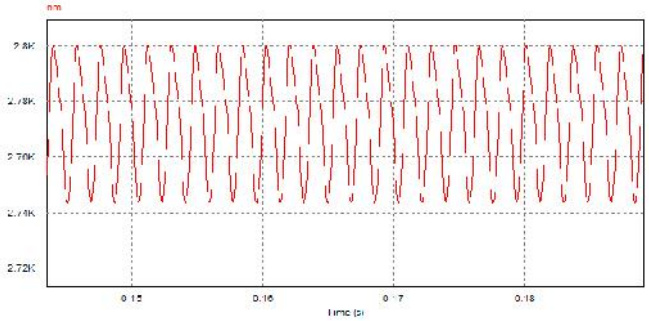

b)

Figure 10. Shaft speed variation, for the new topology of SRM rotor, in the case of a resistant torque of 1 Nm (a) and the ripples of shaft speed curve (b)

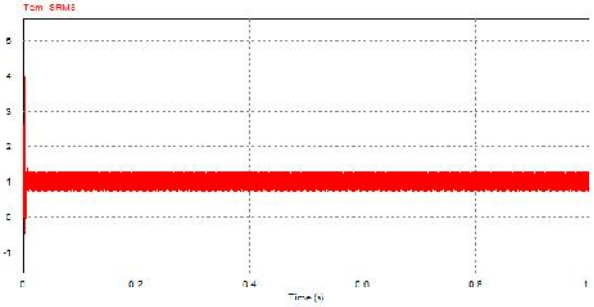

a)

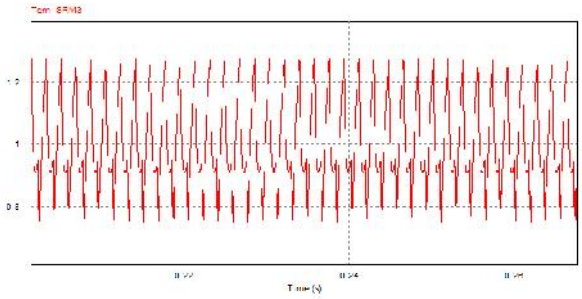

b)

Figure 11. Electromagnetic torque variation, for the new topology of SRM rotor, in the case of a resistant torque of 1 Nm (a) and the ripples of electromagnetic torque curve (b)

C. The case $\frac{L_{\max}}{L_{\min}} = 50$

Fig. 12 and 13 show both speed and electromagnetic torque variations of the new SRM for the same value of the resistant torque of 1Nm and the ripples of these parameters curves for the new inductivities ratio value.

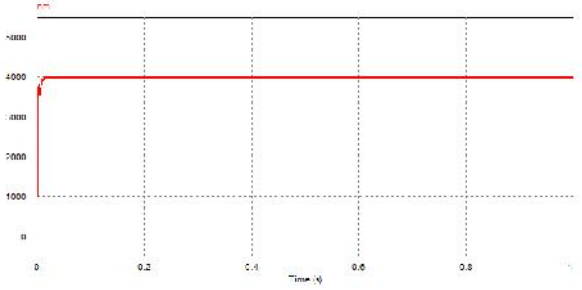

a)

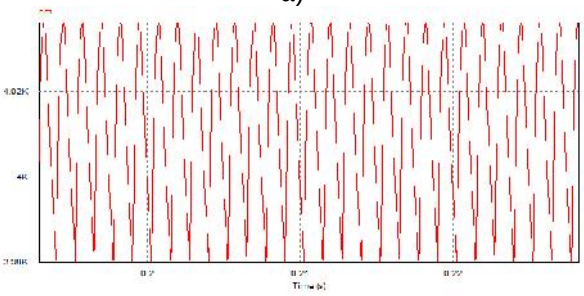

b)

Figure 12. Shaft speed variation, for the new topology of SRM rotor (and the new inductivities ratio), in the case of a resistant torque of 1 Nm (a) and the ripples of shaft speed curve (b)

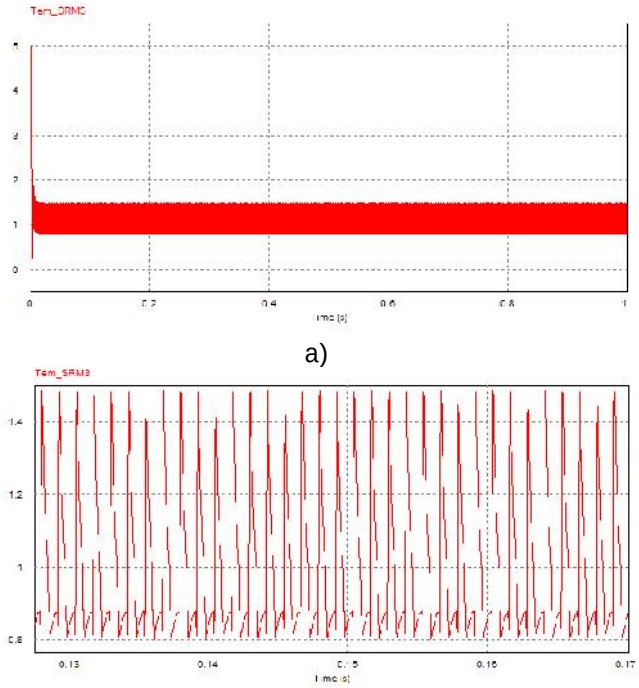

a)

b)

Figure 13. Electromagnetic torque variation, for the new topology of SRM rotor (and the new inductivities ratio), in the case of a resistant torque of 1 Nm (a) and the ripples of electromagnetic torque curve (b)

The simulations performed resulted in the following points:

- strong increase of ratio $L_{\max} / L_{\min}$ value leads to an increase of electromagnetic torque medium value, compared to the reference case (see also Table 1);

- strong increase of ratio $L_{\max} / L_{\min}$ value leads to an increase of energetic efficiency of SRM (Fig. 14);

- unfortunately, although the flutuations of the speed curve in the case of $L_{\max} / L_{\min} = 50$ are, practically, the same as those in the reference case, the flutuations of the electromagnetic torque are twice higher, for this new topology towards the reference case;

- with decrease of the ratio $L_{\max} / L_{\min}$, compared to the reference case, together with shaft load the fluctuations also increase in the shaft speed and electromagnetic torque curves and the energetic efficiency decreases dramatically (Fig. 14).

Table 1

Case	U	I	P_{1ph}	P_{2ph}	P_{3ph}	P_{1t}	T_{load}	T_{emSRM}	n_m	Ω_m	P_2	η_m
-	[V]	[A]	[W]	[W]	[W]	[W]	[Nm]	[Nm]	[rpm]	[rad/s]	[W]	-
$\frac{L_{\max}}{L_{\min}}=10$	162	0.60	28.27	29.02	28.53	85.82	0.1	0.16	7418	776	77.6	0.904
	161	1.27	62	63	62	187	0.5	0.52	3365	352	176	0.941
	161	1.79	90	91	90	271	1	1.01	2361	247	247	0.911
	160	2.53	130	131	130	391	2	2.01	1643	172	344	0.880
	159	3.1	159	160	161	480	3	3.02	1305	137	411	0.856
$\frac{L_{\max}}{L_{\min}}=5$	162	0.9	34.55	35.68	34.71	104.94	0.1	0.18	8750	916	91.6	0.872
	161	1.91	78	80	78	236	0.5	0.52	3964	415	207.5	0.879
	160	2.69	114	116	115	345	1	1.02	2770	290	290	0.840
	159	3.81	169	171	169	509	2	2.03	1913	200	400	0.785
	158	4.81	241	243	242	726	3	3.01	1669	175	525	0.723
$\frac{L_{\max}}{L_{\min}}=50$	162	0.83	48.14	47.89	47.80	143.83	0.1	0.2	12209	1278	127.8	0.888
	161	1.71	104	105	105	314	0.5	0.54	5700	597	298.5	0.950
	160	2.42	151	152	151	454	1	1.04	4005	419	419	0.923
	159	3.41	219	220	219	658	2	2.05	2788	292	584	0.887
	158	4.17	272	274	273	819	3	3.10	2246	235	705	0.860

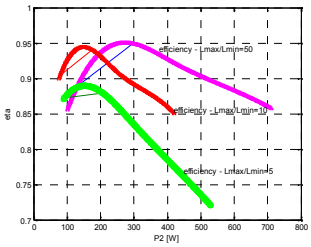

Figure 14. Energetic efficiency of various SRM

Some of the quantities in Table 1 are obtained by calculation so: - the total average power absorbed by the SRM:

$$P_{1t} = \sum_{i-1}^{3} P_{iph} \text{ [W]}, \tag{3}$$

- shaft angular velocity:

$$\Omega_m = \frac{2®n_m}{60} \text{ [rad/s]}, \tag{4}$$

- mechanical shaft power:

$$P_2 = T_{load} \cdot \Omega_m \text{ [W]}, \tag{5}$$

- energy efficiency of SRM:

$$¦_m = \frac{P_2}{P_{1t}}. \tag{6}$$

4. Conclusions

It is worth to state that the strategy adopted in this experiment was to change the SRM rotor topology if the stator armature remains unchanged (and, consequently, the size of motor). Considering this specific characteristic, the conclusions are as follows:

- there is a major influence of SRM inductivities ratio for the two specific positions (alignement, respectively, non-alignement of rotor teeth with the stator armature poles) on the electromagnetic torque and on the energetic efficiency of electromechanic coversion;

- the SRM-ul, by its characteristics, has a special flexibility, and in practice, depending on the nature of application (values of resistant torques, but also the posisioning accuracy requested) may be easily adapted by changing the rotor armature (which would have an adequate topology);

- in order to rise SRM efficiency it is necessary to use mixed strategies (which would combine the different control choices of stator windings with topologic changes of rotor armature);

- the SRMs are used in new applications (such as drive of hybrid motor and electric vehicles, etc.), due to their many advantages [7].

Acknowledgment

This work was supported by a grant of the Romanian National Authority for Scientific Research, CNDI-UEFISCDI, project number PN-II-PT-PCCA-2011-3.2-1680.

References

[1] Jin-Woo Ahn, Switched Reluctance Motor, Torque Control. Prof. Moulay Tahar Lamchich (Ed.), InTech, Available from: http://www.intechopen.com/books/torque-control/switchedreluctance-motor, 2011.

[2]***** Texas Instruments, Switched Reluctance Motor Control – Basic Operation and Example Using the TMS320F240. Application Report SPRA420A - February 2000.

[3] Alexandros M. Michaelides, The design of switched reluctance motors for efficient energy conversion. PhD Thesis, University of Warwick, Coventry, CV4 7AL, September 1994, University of Warwick institutional repository: http://go.warwick.ac.uk/wrap.

[4] Dabija O., Contribuţii privind ameliorarea performanţelor maşinilor cu reluctanţă variabilă. Teză de doctorat, Universitatea Tehnică „Gheorghe Asachi", Iași, 2013.

[5] Ruba M., Design and study of a modular switched reluctance machine. Teză de doctorat, Universitatea Tehnică din Cluj-Napoca, 2010.

[6] **** PSIM, Simulation Software. POWERSYS-France-licence, 2007.

[7] Mehrdad Ehsani, Yimin Gao, Ali Emadi, Modern Electric, Hybrid Electric, and Fuel Cell Vehicles: Fundamentals, Theory, and Design – second Edition. CRC Press, Taylor & Francis Group, USA, 2010.

Addresses:

- Assoc. Prof. Dr. Eng. Ion Voncilă, "Dunărea de Jos" University of Galați, Domnească Street, nr. 47, 800008, Galați, Ion.Voncila@ugal.ro
- Assist. Eng. Răzvan Buhosu, "Dunărea de Jos" University of Galați, Domnească Street, nr. 47, 800008, Galați, Razvan.Buhosu@ugal.ro
- PhD. Eng. Mădălin Costin, "Dunărea de Jos" University of Galați, Domnească Street, nr. 47, 800008, Galați, Madalin.Costin@ugal.ro